IRIS AperTO

UNIVERSITÀ DEGLI STUDI DI TORINO

AperTO - Archivio Istituzionale Open Access dell'Università di Torino

A new UHP unit in the Western Alps: First occurrence of coesite from the Monviso Massif (Italy)

This is a pre print version of the following article:

Original Citation:

Availability:

This version is available http://hdl.handle.net/2318/1924114 since 2024-12-17T08:48:17Z

Published version:

DOI:10.2138/am-2022-8621

Terms of use:

Open Access

Anyone can freely access the full text of works made available as "Open Access". Works made available under a Creative Commons license can be used according to the terms and conditions of said license. Use of all other works requires consent of the right holder (author or publisher) if not exempted from copyright protection by the applicable law.

(Article begins on next page)

07 February 2025

This is the peer-reviewed, final accepted version for American Mineralogist, published by the Mineralogical Society of America.
The published version is subject to change. Cite as Authors (Year) Title. American Mineralogist, in press.
DOI: https://doi.org/10.2138/am-2022-8621. http://www.minsocam.org/

Revision 1

A new UHP unit in the Western Alps: first occurrence of coesite from the Monviso Massif (Italy)

Word Count: 3956

Stefano Ghignone,[1]* Emanuele Scaramuzzo,[2] Marco Bruno,[1] Franz A. Livio.[2]

[1]*Earth Sciences Department, University of Turin, Via Valperga Caluso 35, 10125 Torino, Italy*

[2]*Department of Science and High Technology, University of Insubria, via Valleggio 11, 22100 Como, Italy*

** Corresponding author:* s.ghignone@unito.it

Keywords: coesite, UHP, ophiolite, Monviso, Western Alps

ABSTRACT

The Western Alps are one of the most studied exhumed subduction-accretionary complexes worldwide. Ultra-high pressure (UHP) metamorphism has been documented therein since the 1980's. We now report the first discovery of coesite in the meta-ophiolitic suite of the Monviso Massif, corresponding to the fourth UHP unit defined on the Western Alps. Previous petrographic studies and results from thermodynamic modelling already suggested that these Alpine units may have experienced UHP metamorphism, but no occurrences of index minerals, such as coesite, have been reported to date. The newly discovered coesite inclusions from the Monviso Massif occur as intact single crystals (10-60 μm) hosted by garnet. The observations suggest that they have escaped re-equilibration, and maintained all the original features from the trapping time. The reduced size of the crystals and the lack of re-equilibration significantly differ from the typical textural features

Always consult and cite the final, published document. See http:/www.minsocam.org or GeoscienceWorld

described in past findings (i.e., radial cracks, palisade texture of quartz surrounding coesite relicts). Detailed garnet inclusions analysis and thermodynamic modelling constrained the metamorphic peak conditions at P=2.8-2.9 GPa and T=500-520 °C, within the coesite stability field.

The Lago Superiore Unit represent the fourth UHP unit discovered on the Western Alps. The UHP metamorphism on the Western Alps was considered rare and due to process of unusual units escape from mantle-depth. In our view, the implication of our discovery will take new insight to UHP processes that seems to be more common than expected. Further tectonic reconstructions should take into account the common features observed in the UHP units, for better constrain the subduction- and exhumation-related mechanism that drove the actual stacking of mountain belts.

INTRODUCTION

The ground-breaking finding of natural coesite (SiO_2) in the Western Alps, made by Chopin (1984), revolutionised the geodynamic models of subduction-accretionary complexes. This finding firstly proved that rocks can be subducted to experience mantle conditions (>80 km) and then exhumed (Chopin, 2003; Gilotti, 2013). The discovery of such ultrahigh-pressure (UHP) mineral-bearing rocks also extended the possible depths covered by metamorphic cycles of at least one order of magnitude (e.g., Chopin, 2003) or, alternatively, opened the possibility for invoking non-lithostatic pressure variations (e.g., Tajčmanová et al., 2021).

Despite more than three decades of research in the field of UHP and the reconnaissance of ca. 20 UHP units worldwide (e.g., Gilotti, 2013; Gonzalez et al., 2020), mainly distributed in Phanerozoic subduction-accretionary complexes, the discovery of new UHP units remains a rare event.

This is particularly true for the Western Alps, where only two additional UHP unit has been reported after the very first discovery (Reinecke, 1991; 1998; Frezzotti et al., 2011; Manzotti et al., 2022; **Figure 1a**). Although other direct evidence is lacking, the possible occurrence of other UHP units in the Western Alps has been widely inferred through indirect methods, including thermodynamic modelling and microstructural observations (Angiboust et al., 2012; Gilio et al., 2020; Ghignone et al., 2021). Groppo et al. (2016) further supported the possible attribution of a Western-Alpine origin to unknown-source coesite-bearing rocks unearthed at an archaeological site nearby.

In this paper, we report a new occurrence of intact garnet-inclusions of coesite (10-60 μm) within para-derivative micaschists belonging to the meta-ophiolitic suite of the Monviso Massif (MM) – Western Alps. This discovery constrains the peak pressure conditions reached by the unit within the coesite stability field, and possibly implies that ultrahigh-pressure metamorphism (UHPM) in the Western Alps is more common than expected.

GEOLOGICAL BACKGROUND

The Western Alps (**Figure 1a**) represent part of an exhumed subduction complex (Bousquet et al., 2008; Butler et al., 2013; Schmid et al., 2017) consisting of an assemblage of high (HP) and ultrahigh-(UHP) pressure continent- (Adriatic and European margins) and ocean-derived units (i.e., Piedmont Zone, the former Tethys ocean). The UHP units cropping out in the Western Alps are narrow lens-shaped bodies with a magnitude dimension within the ones of kilometre (Compagnoni and Rolfo, 2003; Groppo et al., 2009; Manzotti et al., 2022) that strongly differ from the hundreds to thousands of kilometres of the Norwegian Caledonides (e.g., Wain 1997) or the Dabie Shan (e.g., Rolfo et al. 2004).

To date, three UHP unit have been recognized with verified observations of UHP mineral assemblages (**Figure 1a** for location): the Brossasco-Isasca (BIU, Chopin 1984) and the Chasteiran units (CU, Manzotti et al., 2022) belonging to the continent derived Dora Maira Massif and the Lago di Cignana Unit (LCU, Reinecke, 1991; 1998) within the ocean-derived Piedmont Zone. The Brossasco-Isasca and the Chasteiran units consist respectively of a polymetamorphic continental basement covered by a monometamorphic metasedimentary succession (e.g., Compagnoni and Rolfo, 2003; Compagnoni et al., 2012) and of thin (few tens of metres thick) graphite-rich, garnet–chloritoid micaschists (Manzotti et al., 2022). The Lago di Cignana Unit is made up of a meta-ophiolitic basement covered by its thin oceanic metasedimentary succession (i.e. eclogite-facies

This is the peer-reviewed, final accepted version for American Mineralogist, published by the Mineralogical Society of America.
The published version is subject to change. Cite as Authors (Year) Title. American Mineralogist, in press.
DOI: https://doi.org/10.2138/am-2022-8621. http://www.minsocam.org/

Piedmont Zone, Groppo et al., 2009; 2019). Peak P–T conditions for the Brossasco-Isasca Unit are in the coesite–eclogite facies (diamond stability field, Hermann, 2003; Groppo et al., 2019): P=4.0-4.3 GPa and T=730 °C. Peak P–T conditions for Lago di Cignana and Chasteiran units are in the coesite-eclogite stability field as well, but at significantly lower Pressure: P=3.2 GPa, T=590-605 °C (Lago di Cignana Unit), P=2.7–2.8 GPa, T= 510–530 °C (Chasteiran Unit).

The Monviso Massif (MM, **Figure 1b**) consists of eclogite-facies units of the Piedmont Zone, constituted by a meta-ophiolitic suite (i.e., serpentinized metaperidotite + Fe-Ti and Mg-Al metagabbro) and covered by a discontinuous metasedimentary sequence. The latter mainly consist of calcschist, with subordinate effusive metabasalt, quartzite, metapelites (i.e. micaschist), mafic paraderivates and grey marbles along the basement\cover transition (e.g., Lombardo et al., 1978; Lombardo et al., 2002; Balestro et al., 2017; Ghignone et al., 2021, De Togni et al., 2021). It is subdivided in two tectono-metamorphic units (**Figure 1b**), which experienced different Alpine HP eclogitic peaks: the Monviso Unit (MU), with P=2.1-2.2 GPa and T=480-500 °C (Angiboust et al., 2012), and the Lago Superiore Unit (LSU), with P=2.6-2.8 GPa and T=530-550 °C (Gilio et al., 2020). For further tectono-stratigraphic subdivision of the Monviso Massif see Balestro et al. (2014).

The Lago Superiore and Lago di Cignana units show similarities in i) the lithostratigraphic setting of the meta-ophiolitic suite, ii) the structural position within the Western Alpine belt, iii) the tectonic and metamorphic relationships with the adjacent units (e.g., Angiboust et al., 2012; Balestro et al., 2017 and references therein).

MATERIAL AND METHODS

The newly discovered coesite-bearing rocks belong to the metasedimentary succession of the Lago Superiore Unit. BR12 sample (object of this study) was collected in the northern sector of the Monviso Massif, at Colle del Baracun (high Pellice Valley; 44°46’23”N; 7°3’44”E; **Figure 1b** for

Always consult and cite the final, published document. See http:/www.minsocam.org or GeoscienceWorld

sample location; see Festa et al., 2015; Balestro et al., 2017 for a more detailed description of the area).

Classical 30 μm-thick sections were used for optical microscope observations, while sections used for μ-Raman investigations and microprobe (SEM-EDS) analysis are 300 μm-thick, doubled polished and uncovered.

SEM-EDS analyses were performed to obtain point data, X-ray and high-resolution multispectral quantitative maps of the entire thin section. Compositional data were collected using a SEM JEOL IT300LV, EDS Oxford Instruments Inca Energy 200, X-act SDD detector. Working conditions were E=15 kV, I probe = 5 nA, EDS process time=1 μs, 10^5 counts/s, livetime= 50 s (data points), dwell time 5 μs, pixel live time 3000 μs, 126 frames (X-ray maps), dwell time 5 μs, pixel live time 400 μs, 226 frames (multispectral map). Multispectral maps (almost 4 x 2 cm) were quantified through Quantmap (Aztec Suite, v.3.3).

Compositional point data were recalculated using the functions proposed by Lanari et al. (2014; 2019).

HORIBA instrument, coupled with a Jobin Yvon HR800 spectrometer and a CCD detector was used for Raman measurements, equipped with a computer-controlled automated X–Y stage. A 532-nm laser was focused onto specimens with a 100X microscope objective (N.A.=0.9) and Raman shifted light was statically dispersed with 1800 groove/mm gratings. The spectrometer was calibrated with a silicon standard. Spectral accuracy and linearity were checked throughout each analytical session by measuring the 520.5 cm^{-1} Raman band of a silicon standard, and the Raman bands of a synthetic quartz reference material. All Raman spectra were acquired for 30 s, 4 repetitions, and measured at room conditions, with a laser spot of 2 μm.

The P–T isochemical phase diagram (pseudosection modelling) approach was applied to the studied sample. Bulk rock compositions (**Table 1**) were calculated by combining the mineral proportions obtained from the quantitative modal estimate of SEM-EDS multispectral map with mineral chemistry. Natural mineral standards were used to calibrate the raw data, by applying the ΦρZ correction (Pouchou and Pichoir, 1988). The multispectral map of the entire thin section was used to derive the effective bulk composition. Point analyses of each phase were recalculated as atoms per formula unit (apfu). Representative SEM-EDS analyses are reported in **Table S1** for garnet (core, mantle and rim), white mica (phengite and muscovite), chloritoid, albite, chlorite and biotite. The fractionation effects on the bulk composition due to the growth of zoned garnet porphyroblasts were considered. In particular, we removed the garnet core composition (5%, see below for details) from the bulk. The pseudosection was then calculated to model the peak P–T conditions of the measured bulk composition (MBC) minus the garnet core. It was computed in the system MnNCKFMASH (MnO-Na_2O–CaO–K_2O–FeO–MgO–Al_2O_3–SiO_2–H_2O) using Perple_X 6.9.1 (Connolly, 1990, 2005, 2009), the internally consistent thermodynamic database of Holland and Powell (2011) and the equation of state for H_2O of Holland and Powell (1998).

Fluid-saturated conditions were assumed, and the fluid was considered as pure H_2O ($aH_2O = 1$). This last assumption is realistic for the studied sample, because of the large occurrence of hydrous phases, and the absence of primary carbonates and sulphides. SiO_2 was considered as normal component (not in excess), because of the low occurrence of quartz both in the matrix and in garnet inclusions. Fe^{3+} was disregarded in the calculated pseudosections, because Fe^{3+}-rich oxides are absent and the amount of Fe^{3+} in the analyzed minerals is negligible. The occurrence of amorphous carbon further confirms low oxidation conditions. However, we investigated the Fe3+ influence on P-T calculation through the realization of isobaric T-X(Fe2O3) and isothermal P-X(Fe2O3) pseudosections, reported in Supporting Information (**Figure S1 and S2**). The following solid solution models were used: chlorite, chloritoid, garnet, white mica (White et al., 2014), clinopyroxene (Green et al., 2007), amphibole (Green et al., 2016). Quartz, lawsonite, kyanite and zoisite were considered as pure phases.

PETROGRAPHY AND μ-RAMAN CHARACTERIZATION

This is the peer-reviewed, final accepted version for American Mineralogist, published by the Mineralogical Society of America.
The published version is subject to change. Cite as Authors (Year) Title. American Mineralogist, in press.
DOI: https://doi.org/10.2138/am-2022-8621. http://www.minsocam.org/

The sample BR12 consists of a coesite-bearing garnet micaschist, collected within the oceanic meta-sedimentary suite (e.g., Festa et al., 2015). The coesite-bearing garnet micaschist outcrop within meter-thick discontinuous metapelitic levels showing different textural features, from fine-graned (**Figure 2a, b**) to conglomeratic (**Figure 2c**) terms.

The analysed lithotype is characterized by a pervasive foliation, mainly defined by white mica, wrapping garnet porphyroblasts (**Figure 3a**). The eclogitic assemblage consists of coesite (<1%), garnet (~10%), phengite (~40%), chloritoid (~1%) and accessory rutile (~6%). Muscovite + paragonite ± biotite and albite + muscovite + paragonite lozenge-shaped pseudomorphs (<1%) after glaucophane and jadeite, respectively (see e.g., Chopin et al., 1991; Groppo et al., 2019), locally occur in fractured garnets (**Figure 3b**). A retrograde mineral assemblage is represented by muscovite (~20%), albite (~10%), chlorite (~4%), biotite (<1%) and accessory titanite (<1%). In addition, minor amounts of amorphous carbon, quartz, apatite, zircon, allanite and opaque iron oxides are observed. The larger garnet porphyroblasts (1-3 mm) hold a microfolded relict foliation defined by amorphous carbon, chloritoid and minor white mica (**Figure 4b**). K-white mica is the most abundant mineral in the sample, showing a strong zoning in phengite (Si = 3.40–3.65 apfu) and muscovite (Si = 3.17–3.33 apfu). Chloritoid (XMg=0.17–0.23) occurs as 100–200 µm sized inclusions within garnet, and is absent in the matrix. Chlorite (XMg=0.52-0.68) and biotite (XMg=0.47-0.58) replace garnet along cracks and rims, but also locally occur in the matrix. Together with paragonite, they also occur within lozenge-shaped pseudomorphs after glaucophane (muscovite + paragonite ± biotite) and jadeite (paragonite + muscovite + albite; **Figure 3b**). Albite (An_{0-6}) is quite abundant in the rock matrix, replacing former paragonite-rich domains. Quartz is rarely present in the rock matrix (~1%). Conversely, quartz and coesite are relatively abundant as inclusions in the garnet (**Figure 3c**). Lawsonite relicts (or paragonite + epidote pseudomorphs after lawsonite) were observed neither in the matrix nor as inclusions in garnet. This observation is confirmed by the very low amount of Ca in the bulk rock (see **Table 1**).

Always consult and cite the final, published document. See http:/www.minsocam.org or GeoscienceWorld

This is the peer-reviewed, final accepted version for American Mineralogist, published by the Mineralogical Society of America.
The published version is subject to change. Cite as Authors (Year) Title. American Mineralogist, in press.
DOI: https://doi.org/10.2138/am-2022-8621. http://www.minsocam.org/

Quantitative X-Ray maps (**Figure 3d, e**) of two selected coesite-bearing garnet porphyroblasts exhibit compositional zoning, characterized by three main concentric shells: a wide core (Alm47-56 Sps32-43 Prp3-5 Grs3-6), a discordant mantle (truncation plane in the syn-tectonic grow of different garnet shells, *sensu* Passcheier and Trouw, 2005, Alm57-74 Sps7-32 Prp4-12 Grs2-6) and a relatively thin discontinuous rim (10-50 μm thick, Alm48-66 Sps16-23 Prp1-9 Grs8h-23). Such concentric shells are well-shown in **Figure 3d**, representing a garnet cut through the core, while in **Figure 3e** a non-equatorial cut through garnet (without the core) is reported. The compositional profiles of the selected garnets are reported in **Figure 3f and 3g**. Spessartine decreases from core to mantle with a typical bell-shaped profile, and then tends to slightly increase at the rim. The opposite trend applies to almandine, which firstly increases and then decreases towards the rim. Pyrope and grossular have relatively low abundances: pyrope slightly increases from core to mantle, whereas it dramatically decreases at the rim; grossular roughly remains constant from core to mantle and increases at the rim (**Figure 3f, 3g**).

Several mineral inclusions are present in the garnet, as detected via μ-Raman and microprobe (**Figure 4a and 4b**; see **Table S1**). SiO_2 polymorphs, amorphous carbon, rutile and zircon were found in each garnet shell. Chloritoid was detected in both the garnet core and mantle, as well as glaucophane and jadeite pseudomorphs. SiO_2 inclusions occur as: i) monomineralic quartz inclusions, ii) polycrystalline quartz inclusions, and iii) monomineralic coesite inclusions. Quartz inclusions consist of 10-80 μm sized isolated crystals within non-fractured or re-equilibrated portions of the garnets. Polycrystalline inclusions are 50-100 μm sized quartz aggregates, surrounded by typical radial cracks filled by quartz and minor chlorite. Coesite inclusions consist of 10-60 μm sized monocrystalline grains surrounded by garnet (few tens of μm below the section surface), with no quartz occurrence at the coesite-garnet interface (**Figure 4c, 4d**). Some inclusions of coesite exhibit well developed facets (**Figure 4c**), while others show a more rounded shape (**Figure 4d**). The presence of coesite is testified by μ-Raman analyses, considering and avoiding possible artefacts or misidentification (Keller and Ague, 2022). The Raman spectra show the typical

Always consult and cite the final, published document. See http:/www.minsocam.org or GeoscienceWorld

This is the peer-reviewed, final accepted version for American Mineralogist, published by the Mineralogical Society of America.
The published version is subject to change. Cite as Authors (Year) Title. American Mineralogist, in press.
DOI: https://doi.org/10.2138/am-2022-8621. http://www.minsocam.org/

peaks of coesite, with a shift of few cm^{-1}. The main peak is located at 522 cm^{-1} (instead of 521 cm^{-1}), and the secondary peaks at 426, 270 and 178 cm^{-1} (**Figure 4e; Table S2**, Boyer et al., 1985). The quartz inclusions hosted in the garnet core are also affected by this shift. The main Raman peak is at 471 cm^{-1} (instead of 464 cm^{-1}), and the secondary peaks occur at 134, 216, 355 and 394 cm^{-1} (**Table S2**).

COESITE-RELATED METAMORPHIC CONDITIONS

The P–T isochemical phase diagram approach was applied to the analyzed sample (see above Material and Methods for details). The pseudosection (**Figure 5**) is dominated by four-to-seven variant fields. Garnet and white mica are predicted to be stable across the whole P–T region of interest; lawsonite is stable at T <480 °C and chloritoid stability field is limited to T<530 °C.

The observed coesite-related mineral assemblage (peak-P) consists of garnet mantle + phengite + glaucophane + jadeite + rutile + coesite, and the vol. % of each modelled phase is reported in **Figure 5**. Glaucophane and jadeite are not preserved, but their former occurrence in the peak-P assemblage is testified by fine-grained pseudomorphs of muscovite + paragonite (± biotite) and paragonite + muscovite + albite, respectively.

The peak-P assemblage covers a relatively narrow P–T range at P>2.7 GPa and T between 490 and 540 °C, above the coesite/quartz transition (**Figure 5**). Further constraints are supplied by the intersection of the compositional isopleths of the garnet mantle (average composition: Alm73Grs4Prp10Sps13), which cross each other in a narrow P–T range, within the garnet + phengite + chloritoid + glaucophane + jadeite + coesite field (2.8–2.9 GPa and 500–520°C, **Figure 5**). The modelled chloritoid compositional isopleths, corresponding to the highest measured XMg values (XMg = 0.20–0.22), cross Grt isopleths in the same P–T range.

Because of the difficulties in assign the measured phengite compositions to a specific generation (i.e. prograde or syn peak-P), the modelled phengite compositional isopleths were not used to further constrain the peak P–T conditions.

Always consult and cite the final, published document. See http:/www.minsocam.org or GeoscienceWorld

This is the peer-reviewed, final accepted version for American Mineralogist, published by the Mineralogical Society of America.
The published version is subject to change. Cite as Authors (Year) Title. American Mineralogist, in press.
DOI: https://doi.org/10.2138/am-2022-8621. http://www.minsocam.org/

The influence of Fe^{3+} on the calculated pseudosection was explored through the calculation of isothermal (**Figure S1**) P–X(Fe2O3) and isobaric (**Figure S2**) T–X(Fe2O3) pseudosections. X(Fe2O3) corresponds to Fe2O3/(Fe2O3+FeO). The P–X(Fe2O3) and T–X(Fe2O3) pseudosections were calculated at 510°C and 2.8 GPa, respectively, that are the P–T conditions estimated for the peak-P in the Fe^{+3}-absent system. Based on the observed stability field of the peak-P assemblage (garnet + phengite + chloritoid + glaucophane + jadeite + coesite) and the garnet and chloritoid isoplets, X(Fe2O3) which can be involved in the bulk is constrained at maximum values lower than 0.05. Overall, the results of the T–X(Fe2O3) and P–X(Fe2O3) pseudosections show that the P–T conditions inferred in the Fe^{+3}-absent system is reliable, as confirmed by direct observation in the mineralogical content.

DISCUSSION

The mineral inclusions preserved in the successive garnet shells reflect the three main metamorphic stages of garnet growth and constrain the (U)HP metamorphic evolution of the Lago Superiore Unit in the northern sector of the Monviso Massif. Quartz, chloritoid and rutile inclusions in the garnet core demonstrate a first prograde stage compatible with HP conditions below the coesite/quartz transition. A second stage, corresponding to the peak-P, with inclusions of coesite, chloritoid and jadeite and glaucophane pseudomorphs in the garnet mantle, indicates UHP conditions above the coesite/quartz transition. A third stage, related to a retrograde path still in HP conditions, corresponds to the growth of garnet rims trapping quartz as inclusions. The pseudosection constrains the peak-P above the coesite/quartz transition, giving P-T conditions of 2.8-2.9 GPa and 500-520 °C (**Figure 5**). These results, now supported by the direct observation of non-re-equilibrated coesite (and polycrystalline quartz after coesite), confirm the Lago Superiore Unit peak P-T estimates above the coesite/quartz transition, previously inferred from thermodynamic modelling only (Angiboust et al., 2012; Gilio et al., 2020). The slight T difference (~30°C) for peak-P conditions, compared with previous P-T estimations for the Lago Superiore Unit (Angiboust

Always consult and cite the final, published document. See http:/www.minsocam.org or GeoscienceWorld

This is the peer-reviewed, final accepted version for American Mineralogist, published by the Mineralogical Society of America.
The published version is subject to change. Cite as Authors (Year) Title. American Mineralogist, in press.
DOI: https://doi.org/10.2138/am-2022-8621. http://www.minsocam.org/

et al., 2012; Gilio et al., 2020), may be the result of the effect of local bulk variations, or to different stable mineral assemblage considered.

Our peak P-T estimation are remarkably similar to those obtained by Manzotti et al. (2022) for the Chasteiran Unit (Dora Maira Massif), outcropping in a lower structural position respect to the meta-ophiolites.

In addition, seen their peak P-T remarkable similarities (**Figure 6**), it is possible to attribute the previously described unknown-source coesite-bearing rocks of Groppo et al. (2016) to the Lago Superiore Unit, despite slight differences in mineralogical composition.

IMPLICATIONS

The “classic” coesite inclusions found in Western Alpine UHP units (e.g., Chopin, 1984; 2003; Reinecke, 1991; 1998) are typically relicts (> 80µm) that have only partially escaped re-equilibration, occurring in polycrystalline quartz, with the typical palisade texture, or inside garnets affected by radial cracks. Conversely, the coesite inclusions found in the Lago Superiore Unit occur as intact single crystals (10-60 µm) hosted by garnet. Possibly, due to their limited size, they escaped re-equilibration and preserved the original features of the trapping time. Similar micro-textures are described in the Lago di Cignana Unit by Taguchi et al., (2021), in the Chasterian Unit by Manzotti et al. (2022) and by Schönig et al. (2022) in detrital coesite-bearing rocks deposed in sedimentary basins worldwide. A consistent shift in the Raman spectra (**Figure 4e** and **Table S1**) is found as a proof of the residual strain preserved in the elastic isolated inclusions (Murri et al., 2018 and references therein).

In this light, the polycrystalline quartz inclusions found in the studied sample are here interpreted as re-equilibrated former coesite inclusions, affected by re-crystallization (i.e., palisade texture) and radial cracks, similar to the ones observed and described in the Brossasco-Isasca, Chasteiran and Lago di Cignana units.

Always consult and cite the final, published document. See http:/www.minsocam.org or GeoscienceWorld

This is the peer-reviewed, final accepted version for American Mineralogist, published by the Mineralogical Society of America.
The published version is subject to change. Cite as Authors (Year) Title. American Mineralogist, in press.
DOI: https://doi.org/10.2138/am-2022-8621. http://www.minsocam.org/

In agreement with the interpretation of Taguchi et al. (2021), we thus infer that the different fate (i.e., preservation or re-equilibration) of coesite inclusions could be influenced by the rheological behaviour of the hosting mineral (e.g., Mazzucchelli et al., 2018; Zhong et al., 2020 and references therein). At the coesite/quartz phase transition, the garnet likely behaved elastically in correspondence of coesite inclusions of small size, while it exhibited a brittle behaviour (i.e., radial cracks) at the contact with larger inclusions. The possible size-dependent preservation fate of inclusions in garnet is a challenging topic and needs further deepening.

Within the tectono-metamorphic Western Alpine evolution, we have now evidence that the UHP peak conditions reached at the Lago Superiore Unit are similar, along the same gradient, to those of the Lago di Cignana Unit (Groppo et al., 2009), located ca. 100 km to the north. Between them, in the Susa Valley, similar peak P-T conditions were calculated for the eclogite-facies meta-ophiolite (SV, Ghignone et al., 2021), though direct coesite (or other UHP minerals) observations are lacking. These units represent detached slices of the down-going Alpine Tethys oceanic slab (i.e. Piedmont Zone), preserving internal stratigraphic coherency, currently tectonically sandwiched within the eclogite-facies meta-ophiolites. This may thus point towards the hypothesis of a dismembered coherent oceanic slab along the whole Western Alps (Bucher et al., 2005; Angiboust et al., 2012; Ghignone et al 2021).

According with Manzotti et al. (2022), the Chasteiran Unit represent a sliced portion of the european continental margin, now stacked within the Dora Maira Massif. The similar peak P-T conditions with the Lago Superiore Unit testifies their similar tectono-metamorphic evolution, likely sharing a common return point.

In this view, the Brossasco-Isasca Unit represents a *unicum* in the Western Alps, due to the strong differences in the peak P-T conditions with respect to the other UHP units.

Newly discovered UHP units will surely renew the interest on debated and poorly understood processes about the formation and the exhumation of UHP units. Their main common feature (i.e.

Always consult and cite the final, published document. See http:/www.minsocam.org or GeoscienceWorld

This is the peer-reviewed, final accepted version for American Mineralogist, published by the Mineralogical Society of America.
The published version is subject to change. Cite as Authors (Year) Title. American Mineralogist, in press.
DOI: https://doi.org/10.2138/am-2022-8621. http://www.minsocam.org/

tiny lens-shaped) will be a crucial observation to take in account for further investigation on the tectonic processes driving the present-day Western Alpine setting.

ACKNOWLEDGMENTS

We thank the editor Claire Bucholz, P. Manzotti and an anonymous reviewer for their critical and constructive reviews. This work was financially supported by PRIN 2017 (2017L83S77), of the Italian Ministry for Education, University and Research (MIUR) of Marco Bruno and by Insubria University Research Fund (FAR) of Franz A. Livio.

Alessia Borghini and Mattia Gilio are warmly thanked for their contribution in the UHP discussion. We are thankful to G. Roberts for his first critical revision of the manuscript and language editing. Special thanks goes to Cinzia and all the staff of the Barbara Lowrie refuge for their hospitality and disponibility during our fieldwork.

REFERENCES CITED

Angiboust, S., Langdon, R., Agard, P., Waters, D., and Chopin, C. (2012) Eclogitization of the Monviso ophiolite (W. Alps) and implications on subduction dynamics. Journal of Metamorphic Geology, 30, 37-61. https://doi.org/10.1111/j.1525-1314.2011.00951.x

Balestro, G., Lombardo, B., Vaggelli, G., Borghi, A., Festa, A. and Gattiglio, M. (2014) Tectonostratigraphy of the northern Monviso Meta-ophiolite Complex (Western Alps). Italian Journal of Geosciences, 133, 409–426. https://doi.org/10.3301/IJG.2014.13

Balestro, G., Festa, A., Borghi, A., Castelli, D., Gattiglio, M., and Tartarotti, P. (2017) Role of Late Jurassic intra-oceanic structural inheritance in the Alpine tectonic evolution of the Monviso meta-ophiolite Complex (Western Alps). Geological Magazine, 155, 233–249, https://doi.org/10.1017/S0016756817000553

Always consult and cite the final, published document. See http:/www.minsocam.org or GeoscienceWorld

This is the peer-reviewed, final accepted version for American Mineralogist, published by the Mineralogical Society of America.
The published version is subject to change. Cite as Authors (Year) Title. American Mineralogist, in press.
DOI: https://doi.org/10.2138/am-2022-8621. http://www.minsocam.org/

Bousquet, R., Oberhänsli, R., Goffé, B., Wiederkehr, M., Koller, F., Schmid, S.M., Schuster, R., Engi, M., Berger, A., and Martinotti, G. (2008) Metamorphism of metasediments in the scale of an orogen: A key to the Tertiary geodynamic evolution of the Alps. In: Siegesmund S., Fügenschuh B. and Froitzheim N. (eds.): Tectonic Aspects of the Alpine-Dinaride-Carpathian System. Geological Society, London, Special Publications, 298, 393-412, https://doi .org/10.1144/SP298.18

Boyer, H., Smith, D.C., Chopin, C., and Lasnier, B. (1985) Raman microprobe (RMP) determinations of natural and synthetic coesite. Physics and Chemistry of Minerals, 12, 45–48, https://doi .org/10.1007/BF00348746.

Bucher K., Fazis Y., De Capitani C., Grapes R. (2005) Blueschists, eclogites, and decompression assemblages of the Zermatt–Saas ophiolite: high-pressure metamorphism of subducted Tethys lithosphere. American Mineralogist, 90, 821–835.

Butler, J.P., Beaumont, C., and Jamieson, R.A. (2013) The Alps 1: A working geodynamic model for burial and exhumation of (ultra) high-pressure rocks in Alpine-type orogens. Earth and Planetary Science Letters, 377, 114–131, https://doi.org/10.1016/j.epsl.2013.06.039.

Chopin, C. (1984) Coesite and pure pyrope in high-grade blueschists of the western Alps: a first record and some consequences. Contributions to Mineralogy and Petrology, 86, 107–118, https://doi.org/10.1007/BF00381838.

Chopin, C. (2003) Ultrahigh-pressure metamorphism: Tracing continental crust into the mantle. Earth and Planetary Science Letters, 212, 1–14, https://doi.org/10.1016/S0012-821X(03)00261-9.

Chopin, C., Henry, C., and Michard, A. (1991) Geology and petrology of the coesite-bearing unit, Dora Maira Massif, Western Alps. European Journal of Mineraology, 3, 263–291, https://doi.org/10.1127/ejm/3/2/0263

Compagnoni, R., and Rolfo, F. (2003) Ultrahigh-pressure units in the Western Alps. in “Ultrahigh-pressure metamorphism”, D.A. Carswell and R. Compagnoni, eds., EMU Notes in

Always consult and cite the final, published document. See http:/www.minsocam.org or GeoscienceWorld

This is the peer-reviewed, final accepted version for American Mineralogist, published by the Mineralogical Society of America.
The published version is subject to change. Cite as Authors (Year) Title. American Mineralogist, in press.
DOI: https://doi.org/10.2138/am-2022-8621. http://www.minsocam.org/

Mineralogy, Eötvös University Press, Budapest, 5, 13–49, https://doi.org/10.1180/EMU-notes.5.2.

Compagnoni, R., Rolfo, F., Groppo, C., Hirajima, T. and Turello, R. (2012) Geological map of the ultra-high pressure Brossasco-Isasca unit (Western Alps, Italy), Journal of Maps, 8 (4), 465-472. https://doi.org/10.1080/17445647.2012.744367

Connolly, J.A.D. (1990) Multivariable phase diagrams: an algorithm based on generalized thermodynamics. American Journal of Science, 290, 666–718.

Connolly, J.A.D. (2005) Computation of phase equilibria by linear programming: A tool for geodynamic modeling and its application to subduction zone decarbonation. Earth and Planetary Science Letters, 236, 524-541.

Connolly, J.A.D., (2009) The geodynamic equation of state: what and how. Geochemistry, Geophysics, Geosystems, 10, Q10014.

De Togni, M., Gattiglio, M., Ghignone, S. and Festa A. (2021). Pre-alpine tectono-stratigraphic reconstruction of the Jurassic Tethys in the High-Pressure Internal Piedmont Zone (Stura di Viù Valley,Western Alps). Minerals, 11, 361. https://doi.org/10.3390/min11040361

Festa, A., Balestro, G., Dilek, Y., and Tartarotti, P. (2015) A Jurassic oceanic core complex in the high-pressure Monviso ophiolite (western Alps, NW Italy). Lithosphere, 7(6), 646-652, https://doi.org/10.1130/L458.1

Frezzotti M.L., Selverstone J., Sharp Z. D., and Compagnoni R. (2011) Carbonate dissolution during subduction revealed by diamond-bearing rocks from the Alps. Nature Geosciences, 4, 703– 706, https://doi.org/10.1038/ngeo1246.

Ghignone, S., Balestro, G., Gattiglio, M., and Borghi, A. (2020) Structural evolution along the Susa Shear Zone: the role of a first-order shear zone in the exhumation of meta-ophiolite units (Western Alps). Swiss Journal of Geosciences, 113(1), 1-16, https://doi.org/10.1186/s00015-020-00370-6

Always consult and cite the final, published document. See http:/www.minsocam.org or GeoscienceWorld

Ghignone, S., Borghi, A., Balestro, G., Castelli, D., Gattiglio, M., and Groppo, C. (2021) HP-tectonometamorphic evolution of the Internal Piedmont Zone in Susa Valley (Western Alps): New petrologic insight from garnet+chloritoid –bearing micaschists and Fe-Ti metagabbro. Journal of Metamorphic Geolology, 39, (4), 391–416, https://doi.org/10.1111/jmg.12574

Gilio, M., Scambelluri, M., Agostini, S.,Godard, M., Pettke, T., Agard, P., Locatelli, M., and Angiboust, S. (2020) Fingerprinting and relocating tectonic slices along the plate interface: Evidence from the Lago Superiore unit at Monviso (Western Alps). Lithos, 352-353, 105308, https://doi.org/doi:10.1016/j.lithos.2019.105308

Gilotti, J.A. (2013) The realm of ultrahigh-pressure metamorphism. Elements, 9, 255–260, https://doi.org/10.2113/gselements.9.4.255

Gonzalez, J.P., Baldwin, S.L., Thomas, J.B., Nachlas, W.O., and Fitzgerald, P.G. (2020) Evidence for ultrahigh-pressure metamorphism discovered in the Appalachian orogen. Geology, 48, 947–951, https://doi.org/10.1130/G47507.1

Green, E.C.R., Holland, T.J.B., Powell, R. (2007). An order-disorder model for omphacitic pyroxenes in the system jadeite-diopside-hedenbergite-acmite, with applications to eclogite rocks. American Mineralogist, 92, 1181–1189.

Green, E. C. R., White, R. W., Diener, J. F. A., Powell, R., Holland, T. J. B., Palin, R. M. (2016). Activity–composition relations for the calculation of partial melting equilibria in metabasic rocks. Journal of Metamorphic Geology, 34, 845–869.

Groppo, C., and Castelli, D. (2010) Prograde P-T evolution of a lawsonite eclogite from the Monviso meta-ophiolite (Western Alps): Dehydration and redox reactions during subduction of oceanic FeTi-oxide gabbro. Journal of Petrology, 51, 2489–2514, https://doi.org/10.1093/petro logy/egq065

Groppo, C., Beltrando, M., and Compagnoni, R. (2009) The P-T path of the ultra-high pressure Lago Di Cignana and adjoining high-pressure meta-ophiolitic units: Insights into the

This is the peer-reviewed, final accepted version for American Mineralogist, published by the Mineralogical Society of America.
The published version is subject to change. Cite as Authors (Year) Title. American Mineralogist, in press.
DOI: https://doi.org/10.2138/am-2022-8621. http://www.minsocam.org/

evolution of the subducting Tethyan slab. Journal of Metamorphic Geology, 27, 207-231, https://doi.org/10.1111/j.1525-1314.2009.00814.x.

Groppo, C., Ferrando, S., Castelli, D., Elia, D., Meirano, V., and Facchinetti, L. (2016) A possible new UHP unit in the Western Alps as revealed by ancient Roman quern-stones from Costigliole Saluzzo, Italy. European Journal of Mineralogy, 28, 1215-1232, https://doi.org/10.1127/ejm/2016/0028-2531.

Groppo, C., Ferrando, S., Gilio, M., Botta, S., Nosenzo, F., Balestro, G., Festa, A., and Rolfo, F., (2019) What's in the sandwich? New P–T constraints for the (U)HP nappe stack of southern Dora-Maira Massif (Western Alps): European Journal of Mineralogy, 31(4), 665–683, https://doi.org/10.1127/ejm/2019/0031-2860.

Hermann, J. (2003) Experimental evidence for diamond-facies metamorphism in the Dora-Maira massif. Lithos, 70, 163–182.

Holland, T.J.B. and Powell, R. (1998). An internally consistent thermodynamic data set for phases of petrologic interest. Journal of Metamorphic Geology, 16, 309–343.

Holland, T.J.B. and Powell, R. (2011). An improved and extended internally consistent thermodynamic dataset for phases of petrological interest, involving a new equation of state for solids. Journal of Metamorphic Geology, 29, 333–383.

Keller, D.S. and Ague, J.J. (2022) Possibilities for misidentification of natural diamond and coesite in metamorphic rocks. Journal of Mineralogy and Geochemistry, 197, (3), 253–261.

Lanari, P., Vho, A., Bovay, T., Airaghi, L., Centrella, S., (2019). Quantitative compositional mapping of mineral phases by electron probe micro-analyser. Geological Society of London, Special Publications, 478, 39-63.

Lanari, P., Vidal, O., De Andrade, V., Dubacq, B., Lewin, E., Grosch, E., Schwartz, S. (2014) XMapTools: a MATLAB©-based program for electron microprobe X-ray image processing and geothermobarometry. Computers and Geosciences. 62, 227-240.

Always consult and cite the final, published document. See http:/www.minsocam.org or GeoscienceWorld

This is the peer-reviewed, final accepted version for American Mineralogist, published by the Mineralogical Society of America.
The published version is subject to change. Cite as Authors (Year) Title. American Mineralogist, in press.
DOI: https://doi.org/10.2138/am-2022-8621. http://www.minsocam.org/

Lombardo, B., Nervo, R., Compagnoni, R., Messiga, B., Kienast, J., Mevel, C., Fiora, L., Piccardo, G., and Lanza, R. (1978). Osservazioni preliminari sulle ofioliti metamorfiche del Monviso (Alpi Occidentali). Rendiconti Societa Italiana Di Mineralogia E Petrologia, 34, 253–305.

Lombardo, B., Rubatto, D. and Castelli, D. (2002) Ion microprobe U-Pb dating of zircon from a Monviso metaplagiogranite: Implications for the evolution of the Piedmont-Liguria Tethys in the Western Alps. Ofioliti, 27, 109-117, https://doi.org/10.4454/ofioliti.v27i2.181.

Manzotti, P., Schiavi, F., Nosenzo, F., Pitra, P. and Ballevre, M. (2022) A journey towards the forbidden zone: a new, cold, UHP unit in the Dora-Maira Massif (Western Alps). Contributions to Mineralogy and Petrology, 177, 59. https://doi.org/10.1007/s00410-022-01923-8

Mazzucchelli, M. L., Burnley, P., Angel, R. J., Morganti, S., Domeneghetti, M. C., Nestola, F., and Alvaro, M. (2018) Elastic geothermobarometry: Corrections for the geometry of the host-inclusion system. Geology, 46(3), 231-234, https://doi.org/10.1130/G39807.1.

Messiga, B., Kienast, J. R., Rebay, G., Riccardi, M. P. and Tribuzio, R. (1999) Cr-rich magnesiochloritoid eclogite from the Monviso ophiolites (Western Alps, Italy). Journal of Metamorphic Geology, 17, 287-299.

Murri, M., Mazzucchelli, M. L., Campomenosi, N., Korsakov, A. V., Prencipe, M., Mihailova, B., Scambelluri, M., Angel, R. J., and Alvaro, M. (2018) Raman elastic geobarometry for anisotropic mineral inclusions: American Mineralogist, 103, (11), 1869-1872, https://doi.org/10.2138/am-2018-6625CCBY.

Passchier, C.W., and Trouw, R.A.J. (2005) Microtectonics, 2nd edn. Springer, Berlin. Pouchou, J. L., and Pichoir, F. (1988). Determination of mass absorption coefficients for soft Xrays by use of the electron microprobe. In D. E. Newbury (Ed.), Microbeam analysis (319–324). San Francisco Press.

Always consult and cite the final, published document. See http:/www.minsocam.org or GeoscienceWorld

Pouchou, J. L., and Pichoir, F. (1988). Determination of mass absorption coefficients for soft Xrays by use of the electron microprobe. In D. E. Newbury (Ed.), Microbeam analysis (319–324). San Francisco Press.

Reinecke, T. (1991) Very-high-pressure metamorphism and uplift of coesite-bearing metasediments from the Zermatt-Saas zone, Western Alps: European Journal of Mineralogy, 3, 7-17, https://doi.org/10.1127/ejm/3/1/0007.

Reinecke, T. (1998) Prograde high- to ultrahigh-pressure metamorphism and exhumation of oceanic sediments at Lago di Cignana, Zermatt-Saas Zone, western Alps: Lithos, 42(3-4), 47-189, https://doi.org/10.1016/s0024-4937(97)00041-8.

Rolfo, F., Compagnoni, R., Wu, X. and Xu, S. (2004) A coherent lithostratigraphic unit in the coesite-eclogite complex of Dabie Shan, China: geologic and petrologic evidence. Lithos, 73, 71–94.

Scaramuzzo, E., Livio, F.A., Granado, P., Di Caupua, A., and Bitonte, R. (2022) Anatomy and kinematic evolution of an ancient passive margin involved into an orogenic wedge (Western Southern Alps, Varese area, Italy and Switzerland). Swiss Journal of Geosciences, 115(1), 1-21, https://doi.org/10.1186/s00015-021-00404-7.

Schmid, S.M., Kissling, E., Diehl, T., van Hinsbergen, D.J.J., and Molli, G. (2017) Ivrea mantle wedge, arc of the Western Alps, and kinematic evolution of the Alps–Apennines orogenic system. Swiss Journal of Geosciences, 110, 581-612, https://doi.org/10.1007/s00015-016-0237-0.

Schönig, J., von Eynatten, H., Meinhold, G., Keno, N., Lünsdorf K. (2022) The sedimentary record of ultrahigh-pressure metamorphism: a perspective review. Earth Science Reviews, 227, 103985.

Taguchi, T., Kouketsu, Y., Igami, Y., Kobayashi, T., and Miyake, A. (2021) Hidden intact coesite in deeply subducted rocks. Earth and Planetary Science Letters, 558, 116763. doi:10.1016/j.epsl.2021.116763.

This is the peer-reviewed, final accepted version for American Mineralogist, published by the Mineralogical Society of America.
The published version is subject to change. Cite as Authors (Year) Title. American Mineralogist, in press.
DOI: https://doi.org/10.2138/am-2022-8621. http://www.minsocam.org/

Tajčmanová, L., Manzotti, P., and Alvaro, M. (2021) Under pressure: high-pressure metamorphism in the Alps: Elements: An International Magazine of Mineralogy, Geochemistry, and Petrology, 17(1), 17-22, https://doi.org/10.2138/gselements.17.1.17.

Wain, A. (1997) New evidence for coesite in eclogite and gneisses: defining an ultrahigh-pressure province in the Western Gneiss region of Norway. Geology, 25, 927–930.

White, R.W., Powell, R., Holland, T.J.B., Johnson, T.E., Green, E.C.R. (2014). New mineral activity-composition relations for thermodynamic calculations in metapelitic systems. Journal of Metamorphic Geology, 32, 261-286.

Whitney, D.L. and Evans B.W., 2010, Abbreviations for names of rock-forming minerals. American Mineralogist, 95(1), 185-187, https://doi.org/10.2138/am.2010.3371.

Zhong, X., Moulas, E., Tajčmanová, L. (2020). Post-entrapment modification of residual inclusion pressure and its implications for Raman elastic thermobarometry. Solid Earth 11, 223-240. https://doi.org/10.5194/se-11-223-2020, 2020

FIGURE CAPTIONS

Figure 1: a) Tectonic map of the Western Alps (modified after Balestro et al., 2017, Ghignone et al., 2020, Scaramuzzo et al., 2022 and Manzotti et al., 2022). Yellow stars indicate UHP coesite-bearing unit locations: Lago di Cignana Unit (LCU), Brossasco-Isasca Unit (BIU) and Chasteiran Unit (CU). Codes: Br: Briançonnais, DM: Dora Maira, GP: Gran Paradiso, MM: Monviso Massif, PF: Penninic Front, SL: Sesia-Lanzo. b) Structural sketch map of the Monviso Massif (MM, modified after Balestro et al. 2017

Figure 2:). Images of the outcropping coe-bearing rocks at the Colle del Baracun. a) Fine-grained Grt-micaschist (44°46'19"N; 7°03'51"E). b) Metaconglomeratic term of the Grt-micaschist

Always consult and cite the final, published document. See http:/www.minsocam.org or GeoscienceWorld

(44°46’23’’N; 7°3’44’’E). c) Detail of the Grt-micaschist at the mesoscale (44°46'19"N; 7°03'47"E). We hope for a respectful behaviour for this outcrop and for the whole area.

Figure 3: a) BSE map of the BR12 section. b) Ab+Ms+Pg pseudomorphs after Jd. c) Microphoto (Plane Polarized Light, PPL) of polycrystalline Qz showing typical palisade texture, with radial cracks, in Grt mantle. d) and e) X-ray maps of two Coe-bearing garnets; map indicates molar percent of spessartine (Xsps). f) and g) Compositional profile of the Grt in d) and e), respectively. Red and yellow stars in all the figures indicate the position of Coe and polycrystalline Qz, respectively. Mineral abbreviations after Whitney and Evans (2010).

Figure 4: a) and b) Microphotos of two Coe-bearing garnets, showing the microstructural position of Coe and other inclusions in each Grt, in Plane Polarized Light (PPL). c) and d) Close-up images in PPL of Coe inclusions in garnet. e) Raman spectra of the Coe inclusions of c) and d), respectively. Peaks marked with the value (cm^{-1}) are assigned to coesite, while peaks marked with asterisk are referred to garnet host mineral. Garnet marked peaks values (Sp80_1 spectrum): 349, 374, 503, 555, 632, 863, 916 and 1041 (cm^{-1}). Please note that 1041cm^{-1} peak is shared between garnet and coesite.

Figure 5: P–T pseudosection modelled for sample BR12 using the measured bulk composition (Table 1) to constrain the P–T conditions for the growth of Grt mantle (peak-P).

Figure 6: Peak P-T conditions of the LSU (1a: Angiboust et al., 2012; 1b: Gilio et al., 2020; 1c: Groppo and Castelli, 2010; 1d: Messiga et al., 1999) compared with LCU (2: Groppo et al., 2009), SV (Susa Valley, 3: Ghignone et al., 2021), CU (4: Manzotti et al., 2022), BIU (5: Groppo et al.,

2019), and the unknown UHP Coe-bearing unit supposed by (6) Groppo et al. (2016). Red square with the star indicates the position of the calculated peak P-T conditions for the LSU in this study.

Table 1: Effective bulk compositions (wt%) used to calculate the pseudosection for the BR12 sample.

MBC = measured bulk composition (wt%); MBC-grt-C = effective bulk composition after fractionation of garnet core										
	Bulk Type	SiO2	Al2O3	FeO	MnO	MgO	CaO	Na2O	K2O	tot
BR12	MBC-pr	64.30	16.02	6.71	0.60	4.91	0.24	1.73	5.49	100.00

This is the peer-reviewed, final accepted version for American Mineralogist, published by the Mineralogical Society of America.
The published version is subject to change. Cite as Authors (Year) Title. American Mineralogist, in press.
DOI: https://doi.org/10.2138/am-2022-8621. http://www.minsocam.org/

Figure 1

Always consult and cite the final, published document. See http:/www.minsocam.org or GeoscienceWorld

This is the peer-reviewed, final accepted version for American Mineralogist, published by the Mineralogical Society of America.
The published version is subject to change. Cite as Authors (Year) Title. American Mineralogist, in press.
DOI: https://doi.org/10.2138/am-2022-8621. http://www.minsocam.org/

Figure 2

Always consult and cite the final, published document. See http:/www.minsocam.org or GeoscienceWorld

This is the peer-reviewed, final accepted version for American Mineralogist, published by the Mineralogical Society of America.
The published version is subject to change. Cite as Authors (Year) Title. American Mineralogist, in press.
DOI: https://doi.org/10.2138/am-2022-8621. http://www.minsocam.org/

Figure 3

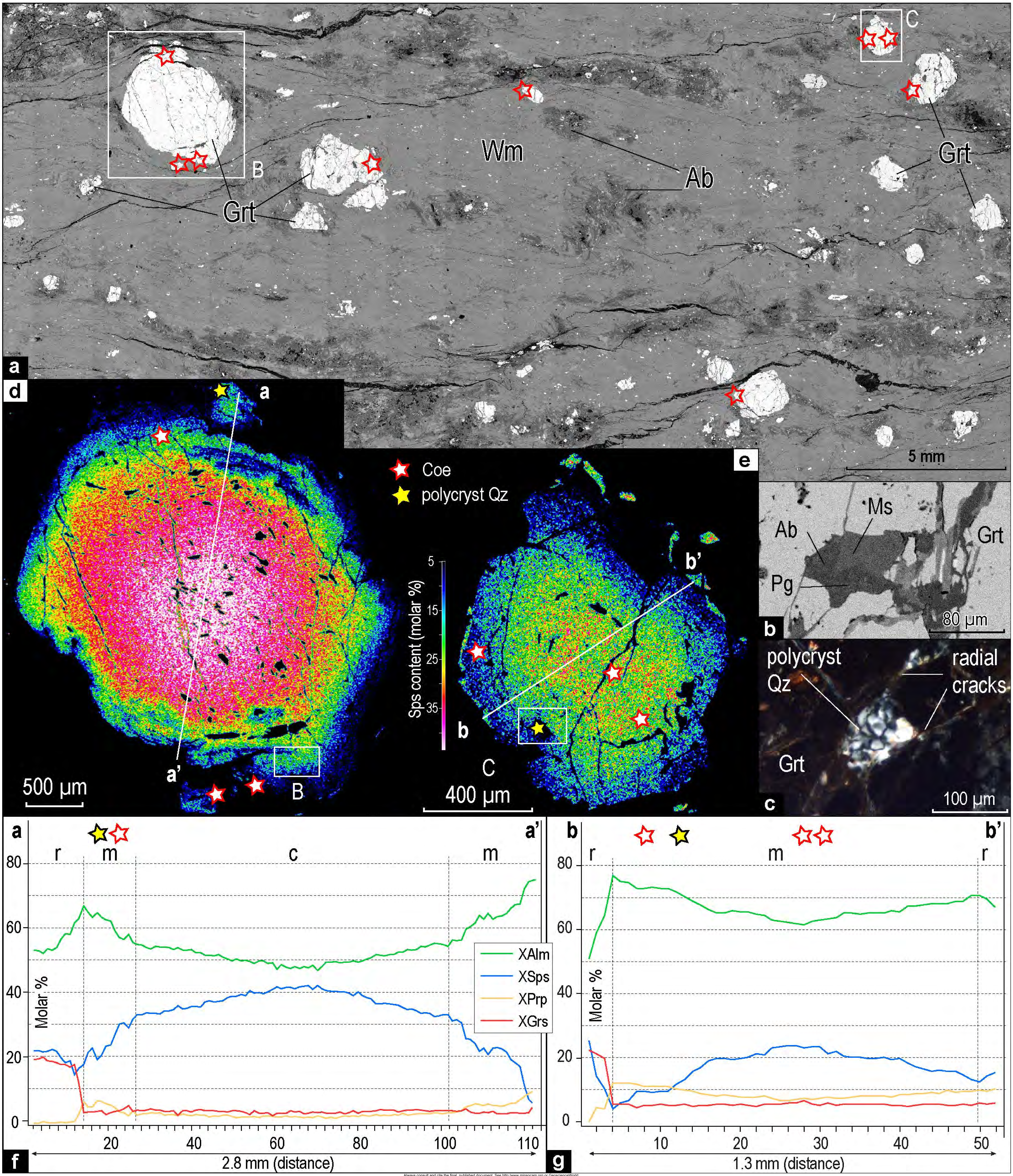

Always consult and cite the final, published document. See http://www.minsocam.org or GeoscienceWorld

This is the peer-reviewed, final accepted version for American Mineralogist, published by the Mineralogical Society of America.
The published version is subject to change. Cite as Authors (Year) Title. American Mineralogist, in press.
DOI: https://doi.org/10.2138/am-2022-8621. http://www.minsocam.org/

Figure 4

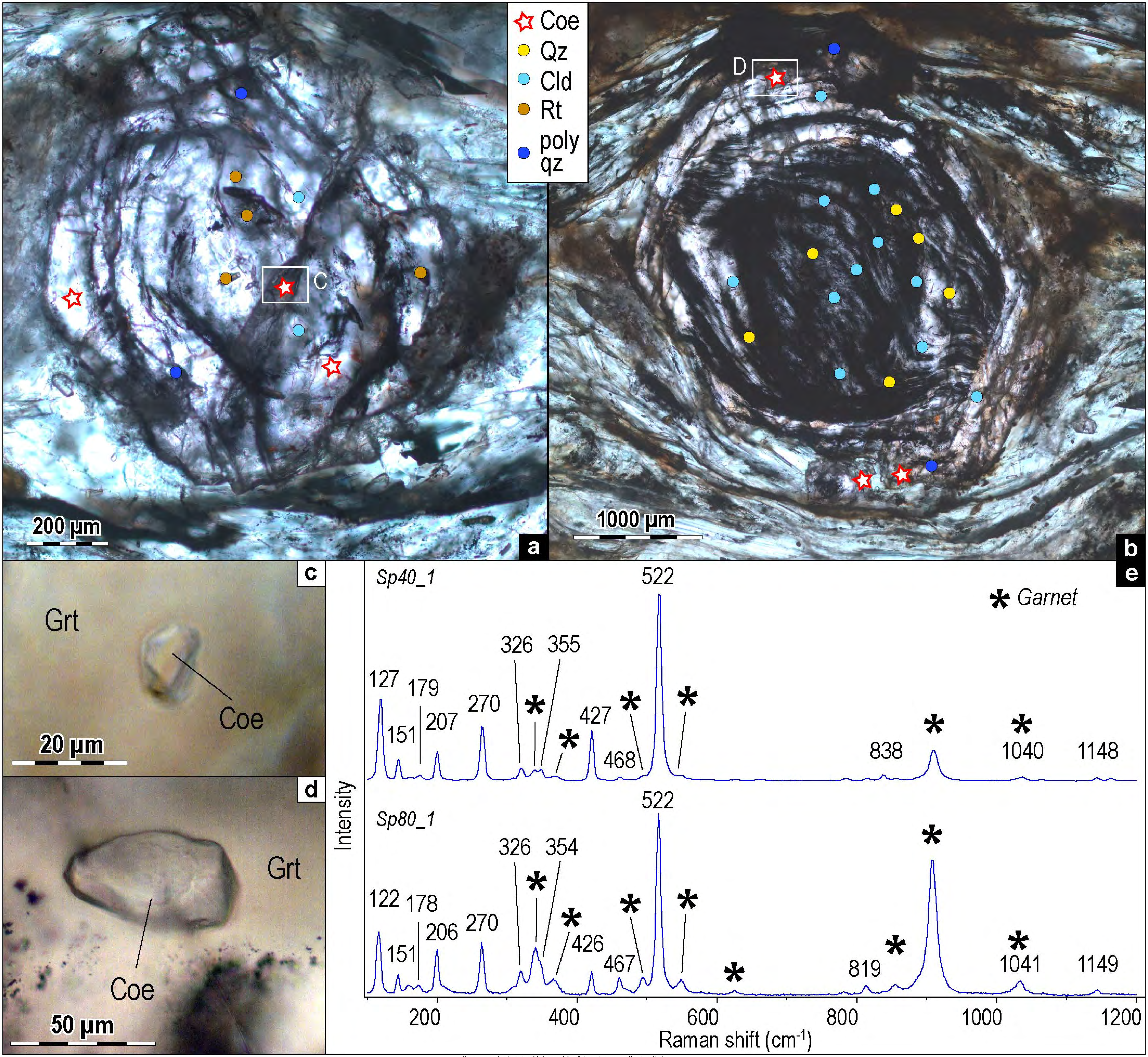

Always consult and cite the final, published document. See http://www.minsocam.org or GeoscienceWorld

This is the peer-reviewed, final accepted version for American Mineralogist, published by the Mineralogical Society of America.
The published version is subject to change. Cite as Authors (Year) Title. American Mineralogist, in press.
DOI: https://doi.org/10.2138/am-2022-8621. http://www.minsocam.org/

Figure 5

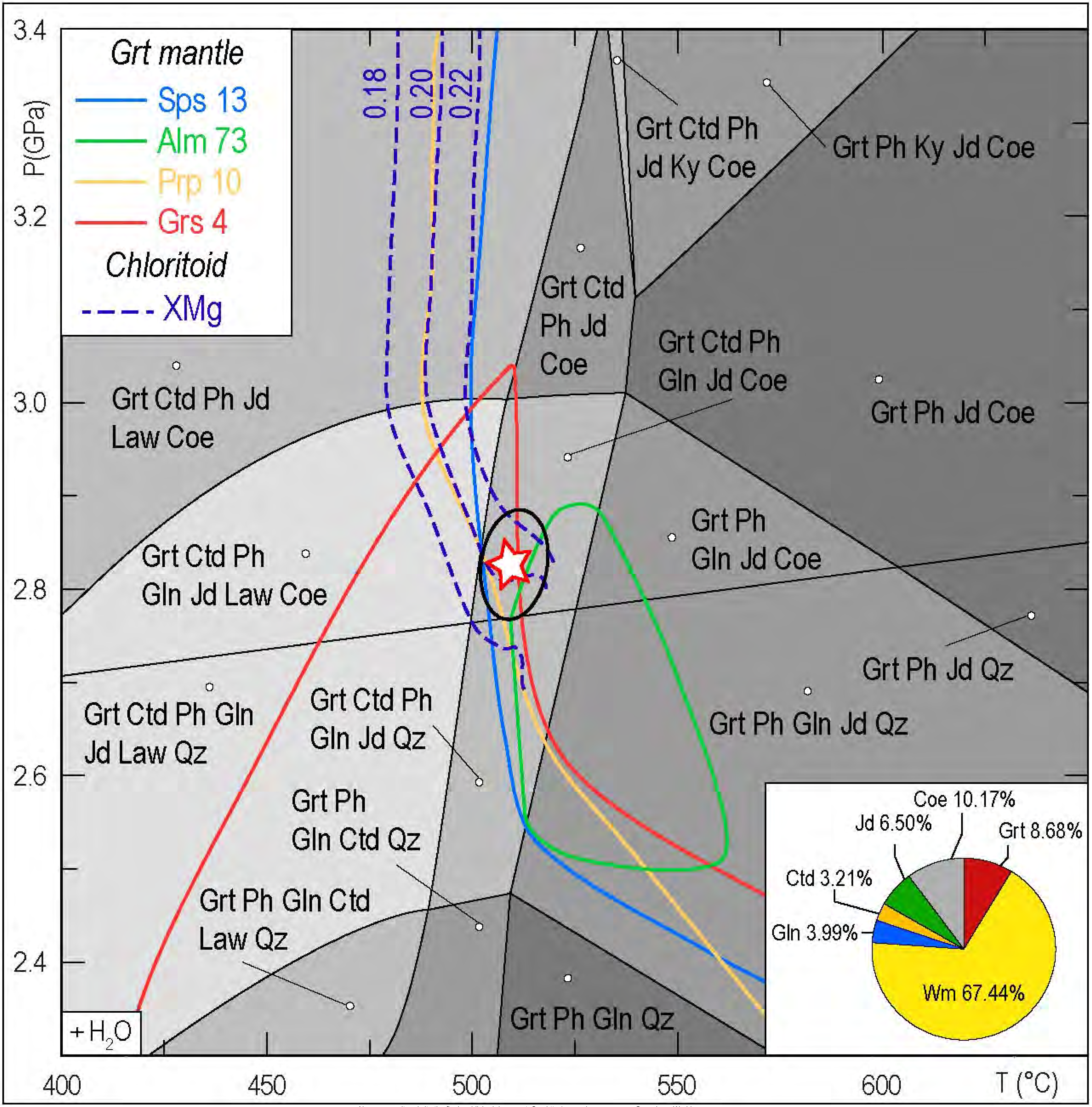

Always consult and cite the final, published document. See http:/www.minsocam.org or GeoscienceWorld

This is the peer-reviewed, final accepted version for American Mineralogist, published by the Mineralogical Society of America.
The published version is subject to change. Cite as Authors (Year) Title. American Mineralogist, in press.
DOI: https://doi.org/10.2138/am-2022-8621. http://www.minsocam.org/

Figure 6

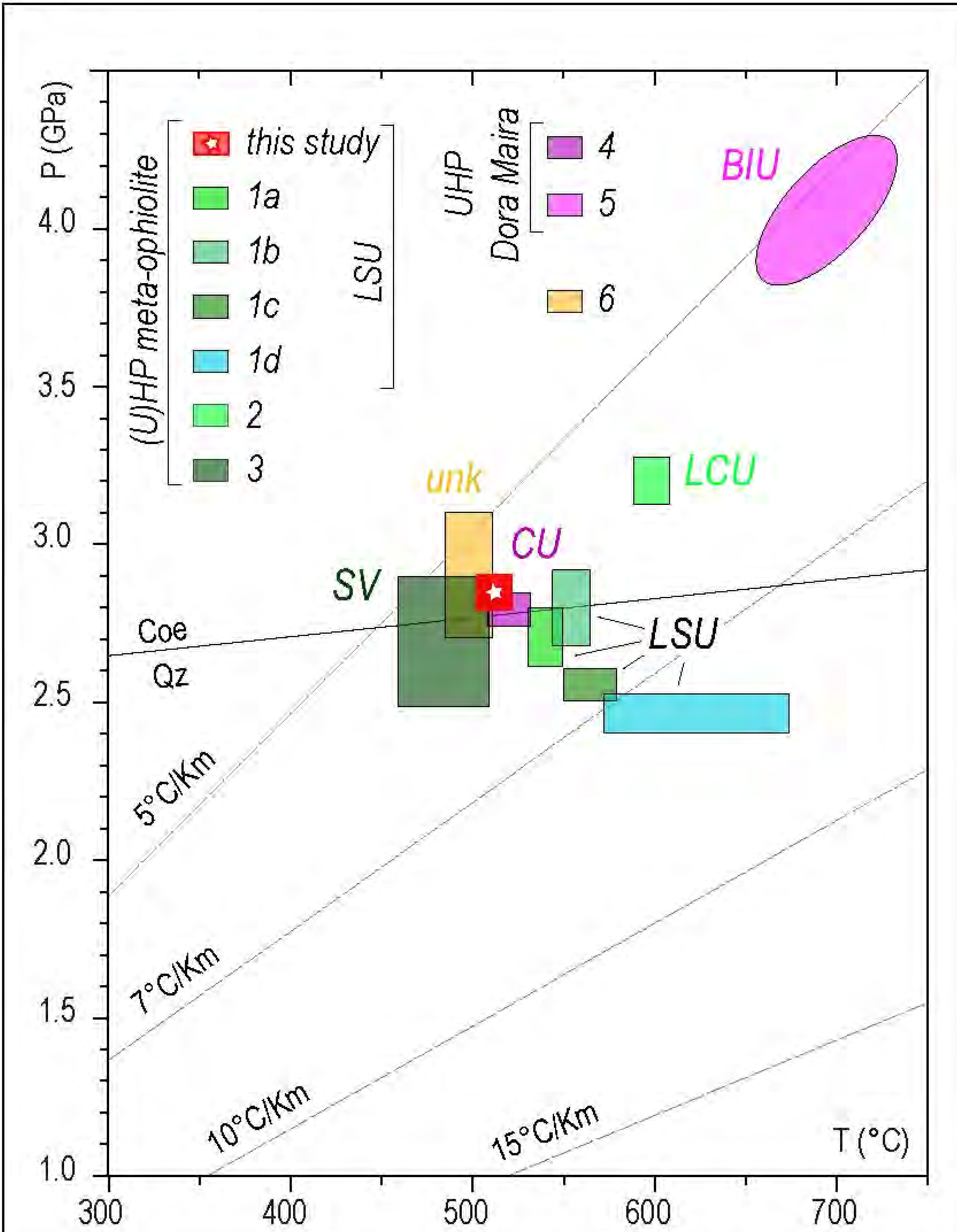

Always consult and cite the final, published document. See http:/www.minsocam.org or GeoscienceWorld